

RESEARCH

Open Access



# Adipose stem cell exosomes promote mitochondrial autophagy through the PI3K/AKT/mTOR pathway to alleviate keloids

Chang Liu<sup>1†</sup>, Liliia Khairullina<sup>1†</sup>, Youyou Qin<sup>1</sup>, Yingbo Zhang<sup>1</sup> and Zhibo Xiao<sup>1\*</sup>

## Abstract

**Background** Fibrosis with unrelieved chronic inflammation is an important pathological change in keloids. Mitochondrial autophagy plays a crucial role in reducing inflammation and inhibiting fibrosis. Adipose stem cell-derived exosomes, a product of adipose stem cell paracrine secretion, have pharmacological effects, such as anti-inflammatory and antiapoptotic effects, and mediate autophagy. Therefore, this study aims to investigate the function and mechanism of adipose stem cell exosomes in the treatment of keloids.

**Method** We isolated adipose stem cell exosomes under normoxic and hypoxic condition to detect their effects on keloid fibroblast proliferation, migration, and collagen synthesis. Meanwhile, 740YPDGFR (PI3K/AKT activator) was applied to detect the changes in autophagic flow levels and mitochondrial morphology and function in keloid fibroblasts. We constructed a human keloid mouse model by transplanting human keloid tissues into six-week-old (20–22 g; female) BALB/c nude mice, meanwhile, we applied adipose stem cell exosomes to treat the mouse model and observed the retention and effect of ADSC exosomes in vivo.

**Results** ADSC exosomes can inhibit the PI3K/AKT/mTOR signaling pathway. The exosomes of ADSCs decreased the inflammatory level of KFs, enhanced the interaction between P62 and LC3, and restored the mitochondrial membrane potential. In the human keloid mouse model, ADSC exosomes can exist stably, promote mitochondrial autophagy in keloid tissue, improve mitochondrial morphology, reduce inflammatory reaction and fibrosis. Meanwhile, At the same time, the exosomes derived from hypoxic adipose stem cells have played a more effective role in both in vitro and in vivo experiments.

**Conclusions** Adipose stem cell exosomes inhibited the PI3K/AKT/mTOR pathway, activated mitochondrial autophagy, and alleviated keloid scars.

**Keywords** ADSCs, Exosomes, Keloids, Mitophagy, PI3K/AKT/mTOR

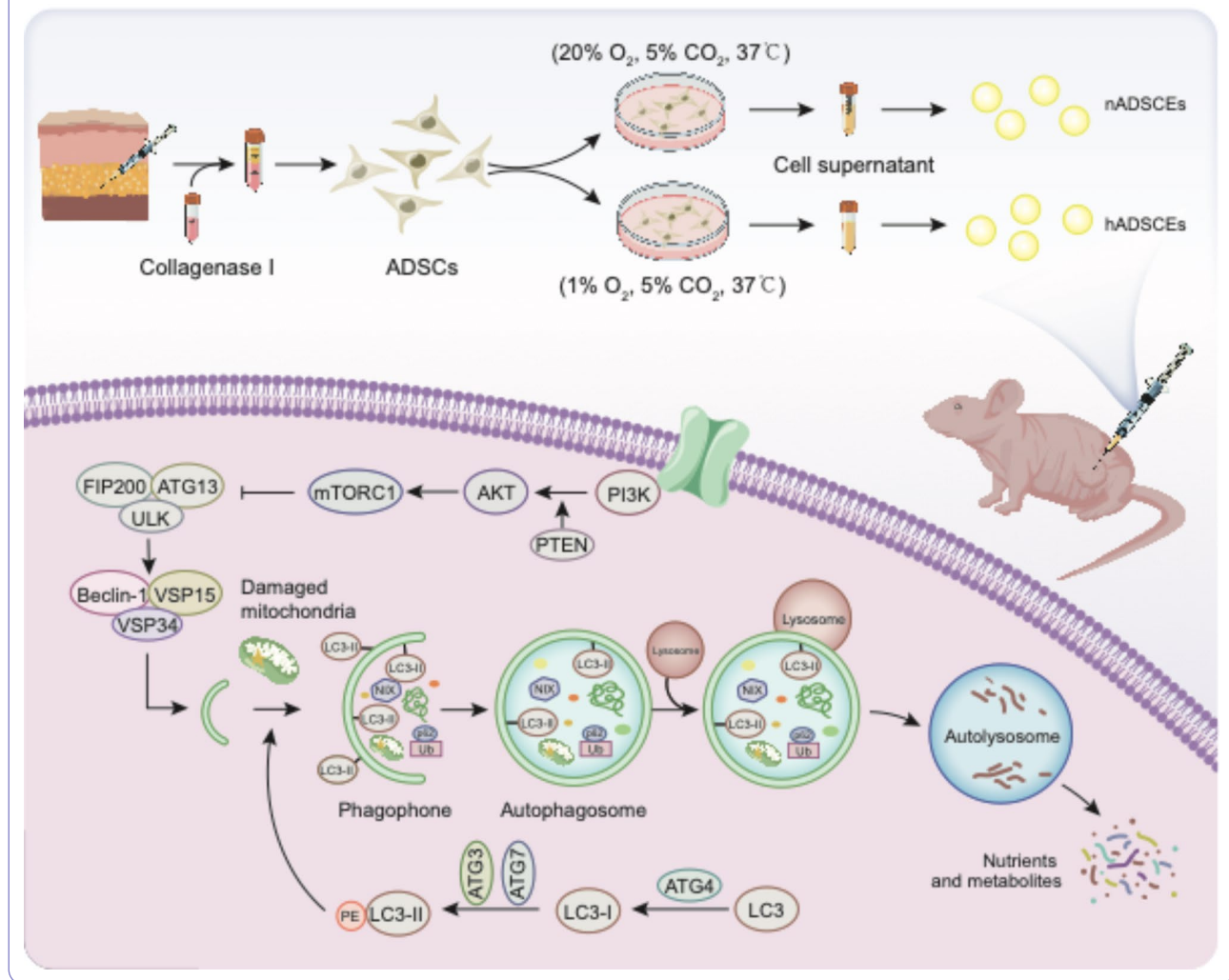
<sup>†</sup>Chang Liu and Liliia Khairullina contributed equally to this work.

\*Correspondence:  
Zhibo Xiao  
Xiaozhibo@doctor@126.com

Full list of author information is available at the end of the article



## Graphical Abstract



## Introduction

Keloids, a fibrotic disorder caused by abnormal wound healing after different skin injuries [1, 2], are characterized by excessive scar tissue formation [3, 4]. During wound healing, the excessive proliferation of fibroblasts and abnormal collagen degradation lead to fibroblast accumulation in the dermis [5]. Chronic inflammation in keloids can activate chronic fibroblast activity and inhibit scar maturation [6]. There are many types of scars, including mature scars, hypertrophic scars and atrophic keloids, among which hypertrophic scars and keloids are the most difficult to distinguish [7]. A remarkable difference between hypertrophic scars and keloids is that keloids often extend beyond the wound, even if there is no skin damage, which will not happen in hypertrophic scars [7]. When keloids are located in visible areas, they are not only aesthetically displeasing but also often cause pain and itching, and when they occur in joints, they can

lead to functional disability [8]. Additionally, in some severe cases, keloids can lead to a serious complication—sepsis [9], due to blockage of the follicular sebaceous glands and sterile inflammation, having psychosocial and quality-of-life implications. There are many treatment options available for individuals with keloids, such as surgical excision, cryotherapy, intralesion injections of medications containing corticosteroids, pulsed dye laser (PDL), fractional lasers, and platelet-rich plasma (PRP) [10, 11]. Currently, corticosteroid injections as one of the most common methods of keloid treatment often result in hypopigmentation and pain during administration, but due to the hyperpigmentation typically seen in keloid lesions, hypopigmentation should be presented as both a potential complication and a treatment goal. Besides, surgical excision alone may result in the formation of similar or larger keloids, cryotherapy may lead to ulceration [8, 12, 13]. Because of these shortcomings, there is still a lack

of effective treatments for keloids; additionally, there is a poor understanding of the mechanisms of keloid formation. Therefore, keloids remain one of the most challenging skin problems.

In adult wound healing, inflammatory cells are recruited to the wound site and promote the synthesis of growth factors [14], such as TGF- $\beta$  and PDGF, which promote fibroblast proliferation and myofibroblast differentiation, as well as the production of a variety of proinflammatory factors (MCP-1, MIP-1, IL-1, and IL-17) that work together to promote extracellular matrix deposition and fibrosis [15, 16]. In fact, the TGF- $\beta$  family is divided into three subtypes. It has been reported that TGF- $\beta$  of the three subtypes are all related to scar formation, but their roles are quite different. Overproduction of TGF- $\beta$ 1 and TGF- $\beta$ 2 may promote scar formation, while TGF- $\beta$ 3 promotes scar-free healing [17]. Autophagy is generally considered to involve the nonselective transport of cytoplasmic components such as nucleic acids, proteins, and organelles to lysosomes and other bulk degradation processes (also referred to as macroautophagy); this process is usually nonselective but also acts as a selective system to mediate the clearance of specific organelles [18]. For example, mitochondrial autophagy targets damaged mitochondria and transports damaged mitochondria to lysosomes [19]. Many studies have demonstrated that when mitochondrial autophagy is reduced, the accumulation of dysfunctional mitochondria can lead to chronic inflammation, the driver of structural abnormalities and dysfunctions of mitochondria observed in many studies. In previous studies, metformin was shown to promote autophagy and restore mitochondrial function while reducing inflammation [20]. Mitochondrial autophagy has been found to be associated with a variety of fibrotic diseases. In pulmonary fibrotic diseases, mitochondrial autophagy is reduced in fibroblasts, excess ROS can regulate the differentiation of fibroblasts to myofibroblasts, and increased mitochondrial autophagy eliminates ROS-producing mitochondria and prevents fibroblasts from differentiating [21]. Additionally, autophagy levels have been shown to be lower in keloids than in normal dermal tissue, and defective autophagy has been shown to prevent the elimination of inflammatory vesicles, leading to excessive inflammation [22]. Many studies have shown that mitochondria in keloid fibroblasts (KFs) are characterized by an abnormal vacuolar, cristae-vanishing morphology [23]. MTOR, including two complexes, mTORC1 and mTORC2, is a key molecule for regulating mitochondrial autophagy, which is closely related to the regulation of mitochondrial function. In PI3K/AKT/mTOR pathway, when PI3K phosphorylation activates AKT, AKT can activate mTORC1 by inhibiting MTOR inhibitor. At the same time, when PI3K phosphorylation activates mTORC2, AKT is activated as the downstream

molecule of mTORC2 and plays a role again to activate mTORC1. When the PI3K/AKT/mTOR pathway is overexpressed, mTORC1 will inhibit the ULK complex and then the VPS34 complex, and finally affect the process of mitochondrial autophagy. Indeed, many studies have shown that PI3K/AKT/mTOR signals are often overexpressed in keloids [24–26]. This suggests that the occurrence of keloid may be related to the abnormal activation of PI3K/AKT/mTOR signal, which leads to the inhibition of mitochondrial autophagy. Overall, mitochondrial autophagy may be a target for the treatment of keloids.

Adipose mesenchymal stem cells (ADSCs) are one of the main sources of extracellular matrix proteins that maintain the structure and function of the skin [27], and these cells interact with skin cells through autocrine or paracrine pathways to regulate the endocytosis and healing processes of the skin, potentially reducing the formation of regenerative scars in wounds by promoting the rebuilding of the extracellular matrix and regulating collagen remodeling [10]. Exosomes are paracrine products of ADSCs and are small membrane vesicle structures with a diameter of 30–150 nm [28]. Exosomes can be internalized by cells to mediate remote intercellular communication and carry complex biological information to target cells. There is growing evidence that ADSC exosomes are involved in a wide range of biological processes by modulating immune and inflammatory responses. In addition, ADSC exosomes reduce reactive oxygen species production and improve mitochondrial function in human umbilical vein endothelial cells (HUVECs) [29]. According to our previous study, compared to the exosomes secreted by ADSCs under normoxic condition (nADSCs), the exosomes secreted by ADSCs under hypoxic condition (hADSCs) were more abundant and exerted greater bioregulatory effects, and there was differential expression of miRNAs between nADSCs and hADSCs [30].

Therefore, we hypothesized that ADSC exosomes could promote mitochondrial autophagy in KFs by regulating the PI3K/AKT/mTOR pathway, restoring mitochondrial bioactivity and alleviating keloid disease and that hADSCs were more effective at treating keloids than were nADSCs.

We first investigated the effects of ADSC exosomes on the growth, survival, migration, collagen synthesis and degree of inflammatory response of KFs *in vitro* by exploring the associated mitochondrial autophagy mechanisms. In addition, we investigated the ability of ADSC exosomes to alleviate keloids in a nude mouse model of subcutaneously embedded human-derived keloid tissue and compared the difference in the role of exosomes under two different culture conditions (nADSCs and hADSCs), providing new information on the role of ADSC exosomes in the treatment of keloids.

## Materials and methods

### Cell culture

Human adipose tissue and keloid tissue samples were aseptically collected from the Department of Plastic and Aesthetic Surgery, Second Affiliated Hospital of Harbin Medical University. These samples were all tested negative for hepatitis C, hepatitis B, syphilis and human immunodeficiency virus tests.

### Cell culture and characterization of ADSCs

ADSCs were isolated according to the procedure detailed in our previous study [30]. Briefly, adipose tissue was minced and digested with type I collagenase, filtered through a strainer and cultured in DMEM/F-12 (Sigma, USA) supplemented with 10% fetal bovine serum (FBS, Corning, USA) and 1% penicillin-streptomycin (Beyotime, China). Osteogenic and adipogenic differentiation were induced in cultured 3rd generation cells, which were stained with alizarin red and oil red O to determine their multidirectional differentiation potential. Subsequently, CD105, CD90, CD45, CD30, and CD29 expression was analyzed by flow cytometry, and ADSCs with good growth characteristics during generation were used in subsequent experiments.

### Keloid fibroblasts (KFs) culture

Keloid tissue was rinsed with PBS and cut it into 2 mm\*2 mm pieces, and the pieces were placed in culture flasks in Dulbecco's modified Eagle medium (DMEM; Gibco, USA) supplemented with 10% fetal bovine serum (FBS; Gibco, USA) and 100 IU penicillin/100 mg/mL streptomycin (Beyotime, China) and cultured at 37 °C in a humidified 5% CO<sub>2</sub> atmosphere. The obtained KFs were used for subsequent experiments.

### Isolation and internalization of exosomes

In order to obtain the exosomes of ADSCs under normoxic condition and anoxic condition (nADSCs and hADSCs), we used a standard incubator (37 °C with 5% CO<sub>2</sub>) and a hypoxic incubator (<1% O<sub>2</sub>) to cultivate ADSCs respectively, and collected the cell supernatant when the cells grew to 70–80% confluence. Exosomes were isolated and purified according to the procedure described in our previous study [30], and the concentration of proteins in the exosomes was measured with a bicinchoninic acid detection kit (Beyotime, China); the exosomes were then stored at 80 °C. The sizes of the purified exosomes ranged from 100 to 150 nm, as determined using a NanoSight LM10 (Malvern Instruments) nanoparticle tracking system. The ultrastructures of the exosomes were analyzed by transmission electron microscopy (TEM) using a Libra 120 instrument (Zeiss). The protein levels of HSP70, TSG101 and CD63 were assessed by western blotting. Exosomes were labeled

using a PKH26 Red Fluorescent Cell Junction Kit (Sigma, USA) according to the manufacturer's instructions. The cell membrane of KFs was labeled using a PKH67 Green Fluorescent Cell Junction Kit (Sigma, USA). KFs were cocultured with exosomes for 24 h. Images were taken under a fluorescence confocal microscope after staining the cell nuclei with DAPI.

### In vitro human KFs treatment

KFs (5×10<sup>6</sup> cells) were treated with nADSCs (100 µg/mL), hADSCs (100 µg/mL), nADSCs (100 µg/mL)+740Y-P (100 µg/mL), hADSCs (100 µg/mL)+740Y-P (100 µg/mL) or PBS (Ctrl), and the cells were harvested after 24 h of treatment and used for subsequent experiments.

### Assessment of cell activity

Cell activity was assessed according to the instructions of an EdU assay kit (Beyotime, China). The treated KFs were incubated with EdU working solution for 2–3 h, after which the cells were fixed and Hoechst (Beyotime, China) staining was applied.

### Analysis of cell migration ability

KFs were seeded into 6-well plates, and when the confluence was 100%, the monolayer was scraped with a 200-µl pipette tip. Serum-free DMEM containing ADSC exosomes (100 µg/ml nADSCs or hADSCs) or PBS was added to the six-well plates. Pictures were taken with a Leica inverted microscope after 0, 12, 24, and 48 h, and migration distances were calculated from the pictures.

Similarly, ADSC exosomes were added to each well of a 24-well plate. KFs were seeded in serum-free medium in the upper chamber of the transwell system. Twenty-four hours later, the cells were stained with 0.1% crystal violet and photographed using a Leica inverted microscope.

### Mitochondrial membrane potential assay

An enhanced mitochondrial membrane potential assay kit with JC-1 (Beyotime, China) was used to assess changes in the mitochondrial membrane potential of KFs. We incubated KFs with JC-1 staining working solution for 20 min at 37 °C according to the manufacturer's instructions, and the cells were subsequently rinsed with staining buffer. The cells were photographed under a fluorescence confocal microscope within 30 min.

### Mitochondrial probe and lysosomal probe staining

The probes MitoTracker Green (Beyotime, China) and LysoTracker Red (Beyotime, China) were applied to label mitochondria and lysosomes in KFs. KFs were incubated with MitoTracker Green or LysoTracker Red for 25–35 min at 37 °C according to the instructions for use,



followed by a wash with PBS. The cells were observed and photographed under a fluorescence confocal microscope.

#### Evaluation of autophagic cells

Cells were transfected with HBAD-mCherry-EGFP-LC3 (HanHeng, China) at an MOI of 500 for 4 h according to the manufacturer's protocol. An equal volume of complete medium was added, followed by incubation for 8 h. Then, the medium was replaced with fresh complete medium, and the cells were incubated for another 24 h. Cells were treated with PBS, nADSCs, hADSCs, or 740YPDGFR as described previously and imaged using a confocal fluorescence microscope.

#### Construction and grouping of keloid animal models

Six-week-old (20–22 g; female) BALB/c nude mice purchased from Weitong Lihua were housed in an IVC system and fed a normal diet. In this experiment, BALB/c nude mice were anesthetized using iso-flurane (1.5–2%) and cervical dislocation was employed for euthanizing the mice. No adverse events occurred in this experiment, and the work has been reported in line with the ARRIVE guidelines 2.0. The sample size of the experimental group and the control group is preliminarily determined according to the previous research on keloids, and each nude mouse is numbered, and one nude mouse is an experimental unit. Using a random number generator, they were randomly divided into three groups: control group (Ctrl), normoxic adipose stem cell exosomes treatment group (nADSCs) and hypoxic adipose stem cell exosomes treatment group (hADSCs). There were 5 nude mice in each group, and 15 nude mice were used in this experiment. At the same time, in order to control the bias of the experiment, the grouping of the experiment was completed by other experimenters who did not understand the research scheme. For humanitarian priority reasons, when animals show anorexia, weakness and other manifestations, they should be removed from the experiment and euthanized in time. No adverse events occurred in this experiment, and no experimental animals or experimental units were excluded. The number of nude mice contributing data for analysis in each experiment is shown in the legend.

Anesthetized BALB/c nude mice were incised to fully expose the right posterior side of the trunk. Keloid tissue was embedded subcutaneously, and the incision was closed. The sutures were removed after 5 days. According to the situation of nude mice, 50  $\mu$ l of nADSCs, hADSCs or PBS was injected around the embedded tissue every other day, starting on postoperative day 7. Photographs were taken on days 0, 7, 14, and 21, and the keloid tissue transplanted under the skin was harvested and weighed on day 21 and used for the subsequent experiments.

#### HE staining and Masson staining

Keloids in the mice were isolated, weighed and fixed in 4% paraformaldehyde solution. After 48 h of fixation, keloids were embedded in paraffin and sectioned. Subsequently, hematoxylin-eosin (H&E) staining and masson staining was performed, and images were obtained with a Leica microscope.

#### Immunofluorescence staining

To observe mitochondrial autophagy in keloids, keloid sections were placed in goat serum and incubated for 1 h. Subsequently, the sections were incubated with anti-LC3II and anti-TOMM20 primary antibodies at 4 °C overnight. The sections were rinsed and then incubated with secondary antibody for 1 h, stained with DAPI, and visualized under a fluorescence confocal microscope.

#### Transmission electron microscopy

Keloids or exosomes were fixed in 2.5% glutaraldehyde for 24 h and dehydrated using different concentrations of ethanol and acetone. The dehydrated tissues were stained with uranyl acetate and lead citrate and then viewed under a transmission electron microscope.

#### Statistical analysis

All experiments were repeated at least 3 times, and the results are expressed as the mean  $\pm$  standard deviation. Student's t test was used for intergroup comparisons, and one-way analysis of variance (ANOVA) was used for multigroup comparisons, with differences considered statistically significant at  $P < 0.05$  (\* $P < 0.05$ ; \*\* $P < 0.01$ ; \*\*\* $P < 0.001$ , \*\*\*\* $P < 0.0001$ ). The statistical analyses and generation of images were performed with GraphPad Prism 9.0.

## Results

#### Characterization of ADSCs

To obtain ADSCs, adipose stem cells were isolated from the abdominal adipose tissue of liposuction patients. In the 5th generation of ADSCs, ADSCs were induced to differentiate into osteoblasts and adipocytes, and lipid droplets and calcium nodules were stained with oil red O and alizarin red, respectively, to indicate their multi-differentiation potential for osteoblastogenesis and lipogenesis (Fig. 1A, B). Moreover, according to the flow cytometry results, ADSCs were positive for CD105, CD90, and CD29 expression and negative for CD45 and CD30 expression (Fig. 1C). These results were consistent with the characterization of ADSCs in previous studies, indicating that ADSCs were successfully isolated.

#### Characterization and internalization of ADSC exosomes

To explore the differences in the effects of ADSC exosomes on keloids under different culture conditions,

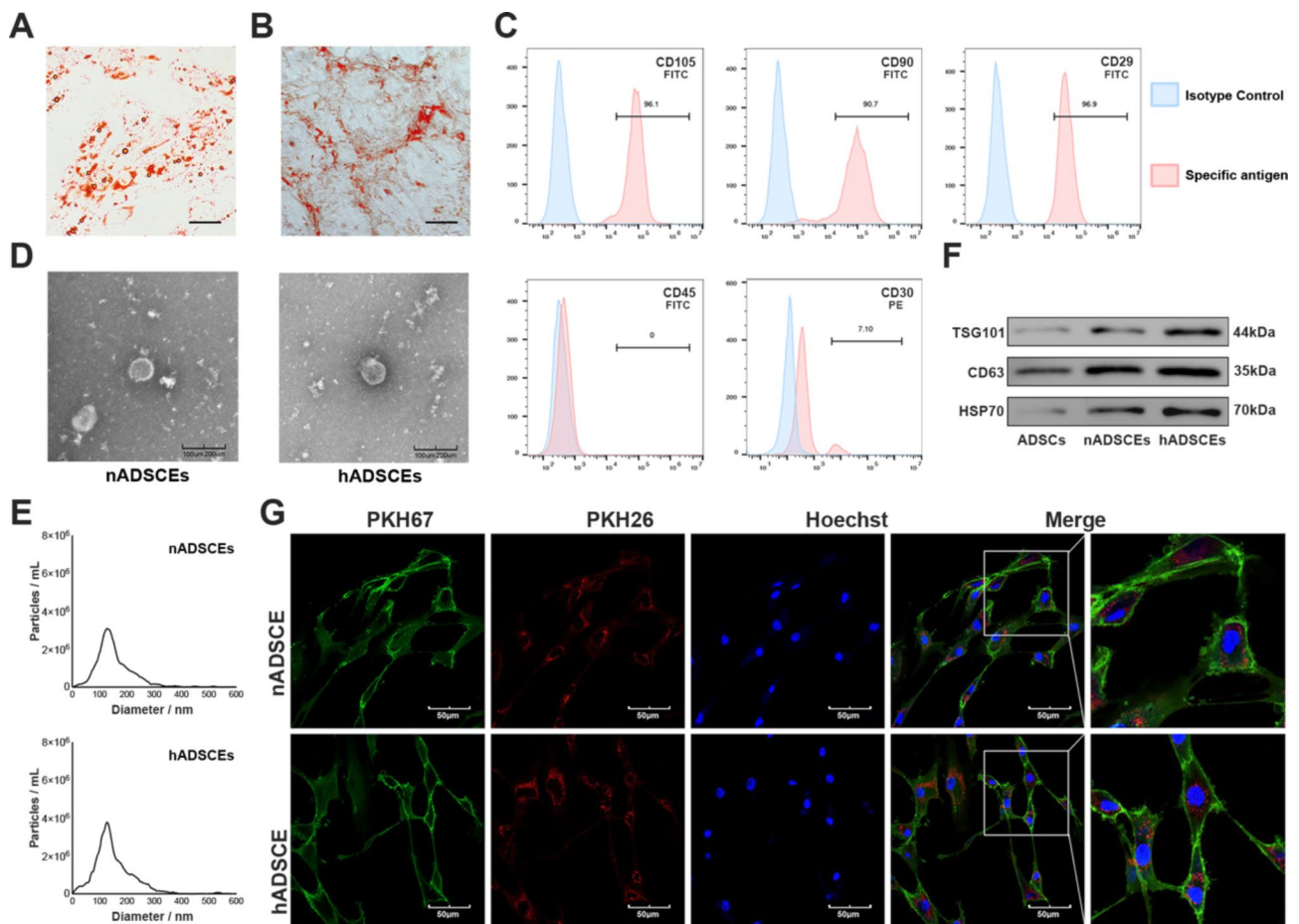


**Fig. 1** ADSCs and ADSC exosomes. **(A)** ADSCs that were able to differentiate into adipocytes were stained with Oil Red O to detect lipid droplets. **(B)** Calcium nodules stained with Alizarin Red S are shown, indicating that ADSCs could differentiate into osteoblasts. **(C)** Flow cytometry analysis of hADSC-specific antigen labeling. **(D)** Morphology of nADSCs and hADSCs under electron microscopy. **(E)** Particle size distributions of nADSCs and hADSCs. **(F)** Western blot analysis of the surface markers of nADSCs and hADSCs. **(G)** Fluorescence images of PKH26-labeled nADSCs and hADSCs internalized by PKH67-labeled KFs. Full-length blots are presented in Supplementary Fig. 1

exosomes were isolated from ADSCs cultured under normoxic and hypoxic condition (nADSCs and hADSCs). Electron microscopy revealed that both types of exosomes had circular vesicle-like structures with lipid bilayers (Fig. 1D). The size distribution of the total extracts ranged from 150 to 200 nm, which was consistent with the characteristics of exosomes (Fig. 1E). Moreover, western blot results revealed the positive expression of exosome marker proteins such as TSG01, CD63 and HSP60 in nADSCs and hADSCs, with the expression of these markers being significantly higher in hADSCs than in nADSCs, which indicated that ADSC exosomes were successfully isolated and that ADSCs secreted more exosomes under hypoxic condition (Fig. 1F). The exosomes were labeled with fluorescent PKH26 to identify nADSCs and hADSCs and fluorescent PKH67 to identify KFs for 24 h and then photographed under a fluorescence confocal microscope (Fig. 1G). The results showed that

nADSCs and hADSCs were successfully internalized by KFs.

#### In vitro, ADSC exosomes inhibited the proliferation and migration of KFs

To determine the effect of ADSC exosomes on KFs in an in vitro environment, nADSCs and hADSCs were cocultured with KFs, followed by incubation with EdU to assess KFs activity (Fig. 2A), and a scratch test and a transwell test were used to assess hKF migration (Fig. 2B, C). The results showed that ADSC exosomes significantly inhibited the proliferation and migration of KFs and that the effect of hADSCs was greater than that of the nADSCs.

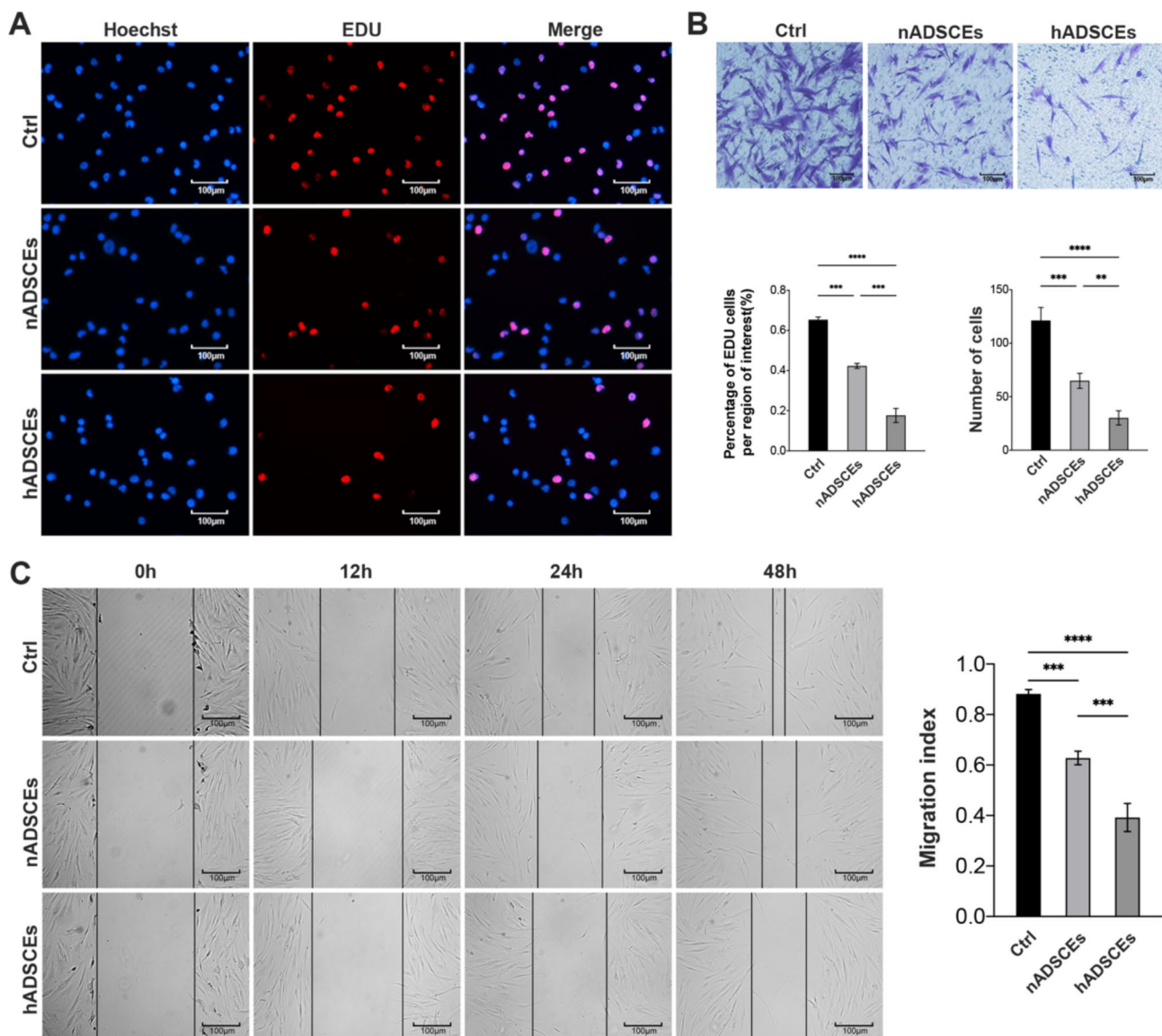


**Fig. 2** Compared to nADSCs, hADSCs significantly inhibited the proliferation and migration of KFs. **(A)** Cell proliferation analyzed by EdU. **(B, C)** Determination of the migration capacity of KFs by scratch test and transwell test

### In vitro, ADSC exosomes can inhibit PI3K/AKT/mTOR pathway and alleviate chronic inflammation caused by scar formation and fibrosis

To assess the correlation between the effect of ADSC exosomes on KFs and the PI3K/AKT/mTOR pathway, we cocultured KFs with ADSC exosomes and pretreated the cells with 740Y-P. The results showed that the PI3K/AKT/mTOR pathway in KFs was significantly inhibited by the action of ADSC exosomes (Fig. 3A). Moreover, RT-PCR analysis of KFs treated with ADSC exosomes indicated a significant decrease in the expression of the inflammatory factors TGF- $\beta$ 1, TNF- $\alpha$ , IL-6, and IL-10 (Fig. 3B). Western blot analysis of collagen deposition and fibrosis levels revealed a significant decrease in

COL1, COL3, and  $\alpha$ SMA expression (Fig. 3C). Similar to previous results, the effect of hADSCs was greater than that of nADSCs. ADSC exosomes were significantly inhibited in the 740Y-P-pretreated KFs. Thus, ADSC exosomes inhibited chronic inflammation and attenuated collagen deposition and fibrosis in KFs, possibly through the PI3K/AKT/mTOR pathway.

### In vitro, ADSC exosomes promote mitochondrial autophagy and restore mitochondrial structure and function

Mitochondrial autophagy is a type of autophagy that removes damaged mitochondria by selectively transporting them to lysosomes. The observation of the formation

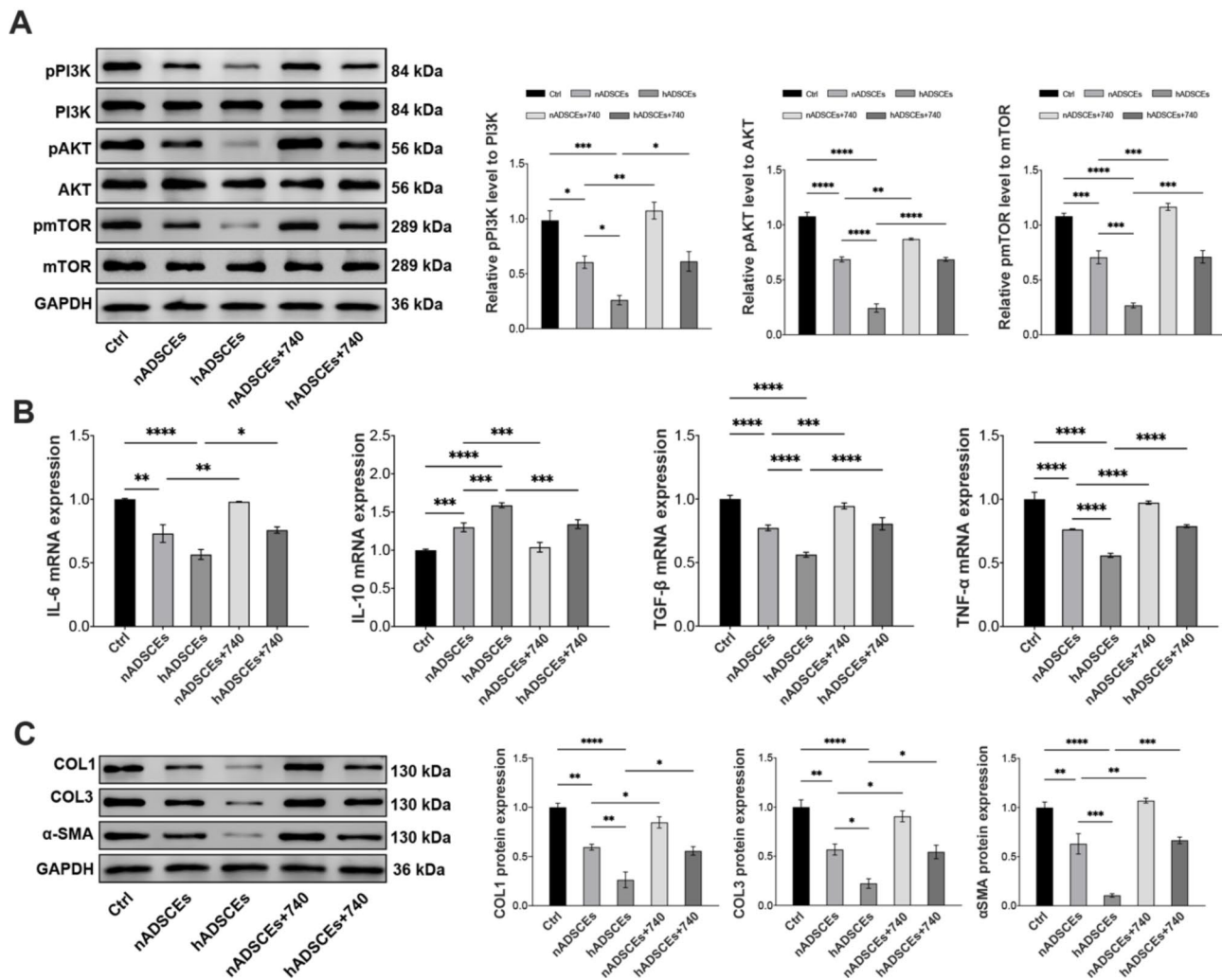


**Fig. 3** ADSC exosomes inhibit the phosphorylation of components of the PI3K/AKT/mTOR pathway, attenuate inflammation, and inhibit collagen deposition and fibrosis. **(A)** Western blot analysis of PI3K/AKT/mTOR pathway protein expression levels. **(B)** RT-PCR was used to analyze the expression levels of the inflammatory factors IL-6, and IL-10, TGF-β1 and TNF-α. **(C)** The protein expression levels of COL1, COL3, and αSMA in treated KFs were analyzed. Full-length blots are presented in Supplementary Fig. 2. The data are expressed as the mean ± standard deviation.  $n = 5$ . \* $P < 0.01$ , \*\* $P < 0.001$ , \*\*\* $P < 0.0001$

of autophagosomes and autolysosomes through transfection with fluorescent mRFP-GFP-LC3 showed that the level of autophagic flow was enhanced in KFs in response to ADSC exosomes (Fig. 4A). The JC-1 staining results showed that the mitochondrial membrane potential was restored (Fig. 4B). Therefore, it is reasonable to speculate that the increased autophagic flux in KFs may affect their mitochondrial structure and function and that ADSC exosomes may promote mitochondrial autophagy in KFs. Therefore, we applied a mitochondrial probe and a lysosomal probe to stain the mitochondria and lysosomes of KFs and measured the length of the mitochondria and the colocalization of mitochondria and lysosomes (Fig. 4C). The results showed that the mitochondrial length increased and that the colocalization coefficients of mitochondria and lysosomes increased in the presence of ADSC exosomes. Western blot results showed

that ADSC exosomes decreased the expression level of Beclin1, increased the levels of P62 and LC3II/LC3I and promoted autophagy in KFs, while the expression of HSP60 and Tomm20 decreased, suggesting a decrease in mitochondrial number (Fig. 4D). Moreover, when 740Y-P was applied, the ability of ADSC exosomes to promote the autophagic flow of KFs and restore mitochondrial morphology and function was suppressed (Fig. 4D). These results suggest that ADSC exosomes may promote mitochondrial autophagy in KFs and restore mitochondrial structure and function through the PI3K/AKT/mTOR pathway.

#### ADSC exosomes significantly attenuate pathology and clinical signs in keloid model mice

We established a keloid implantation mouse model using fresh human keloid tissue and BALB/c nude mice,



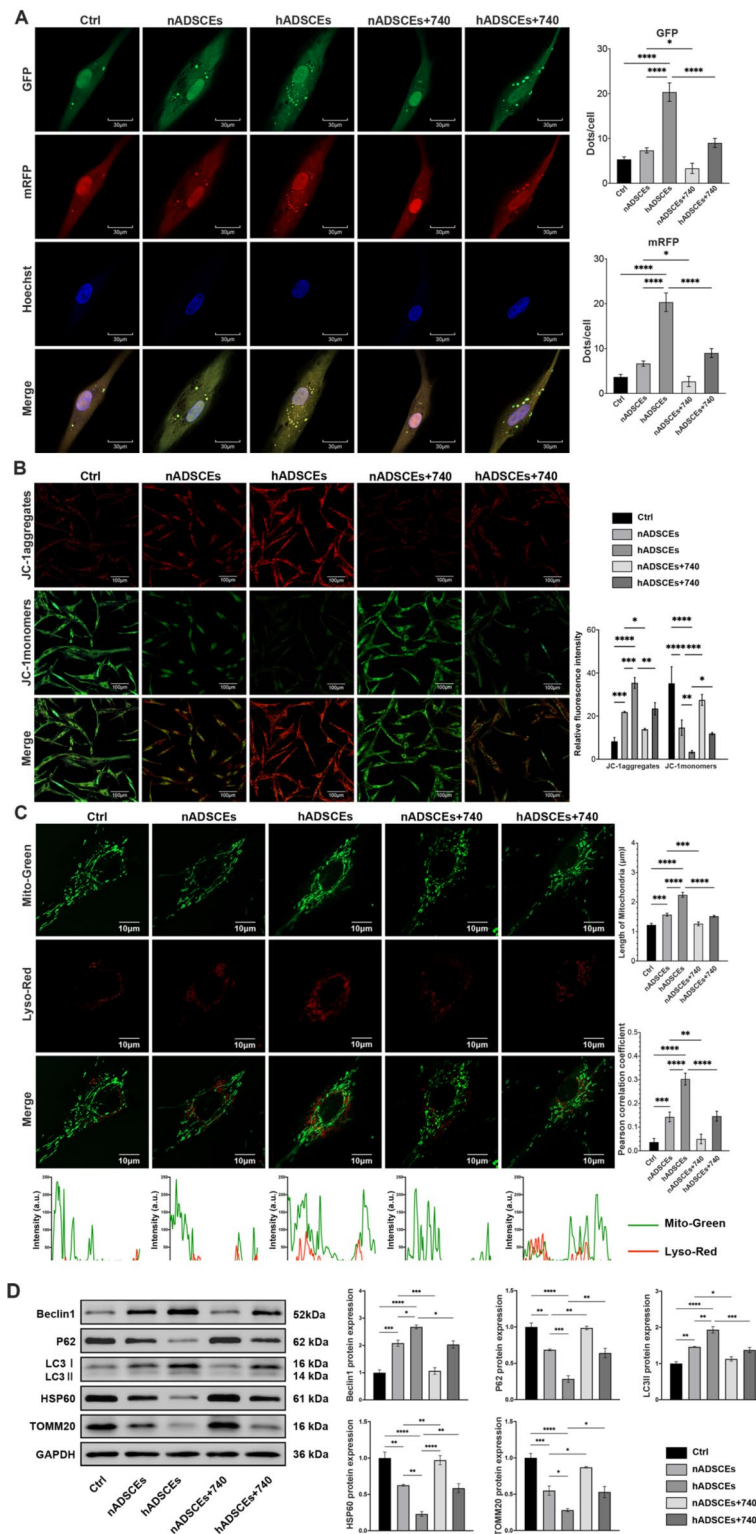


**Fig. 4** Effect of ADSC exosomes on autophagy and mitochondria in KFs. **(A)** Confocal microscopy was used to observe the formation of autophagosomes and autolysosomes after the transfection of KFs with fluorescent mRFP-GFP-LC3. **(B)** JC-1 staining and confocal microscopy were used to observe changes in the mitochondrial membrane potential. **(C)** After staining with a mitochondrial probe and lysosomal probe, confocal microscopy was used to observe mitochondrial morphology and calculate the colocalization coefficients of mitochondria and lysosomes. **(D)** Western blot analysis of the protein expression levels of Beclin1, P62, LC3, HSP60 and TOMM20. Full-length blots are presented in Supplementary Fig. 3

injected nADSCs and hADSCs every other day for 7 days, and removed keloid grafts after 27 days to evaluate the effect of the ADSC exosomes on keloid progression in vivo (Fig. 5A). ADSC exosomes were stained with DIR, and animal imaging system showed that they were absorbed by keloid tissue (Fig. 5B). In addition, we labeled ADSC exosomes with PKH26 and injected them

into the keloid tissue of mouse model, and observed the retention of A in keloid tissue after 7 days (Fig. 5C). To visualize the pathological changes in keloid tissue after treatment with ADSC exosomes, we performed HE and Masson staining. In the control group, the keloid tissue contained many coarse collagen bundle aggregates; after treatment, there was a significant decrease in these

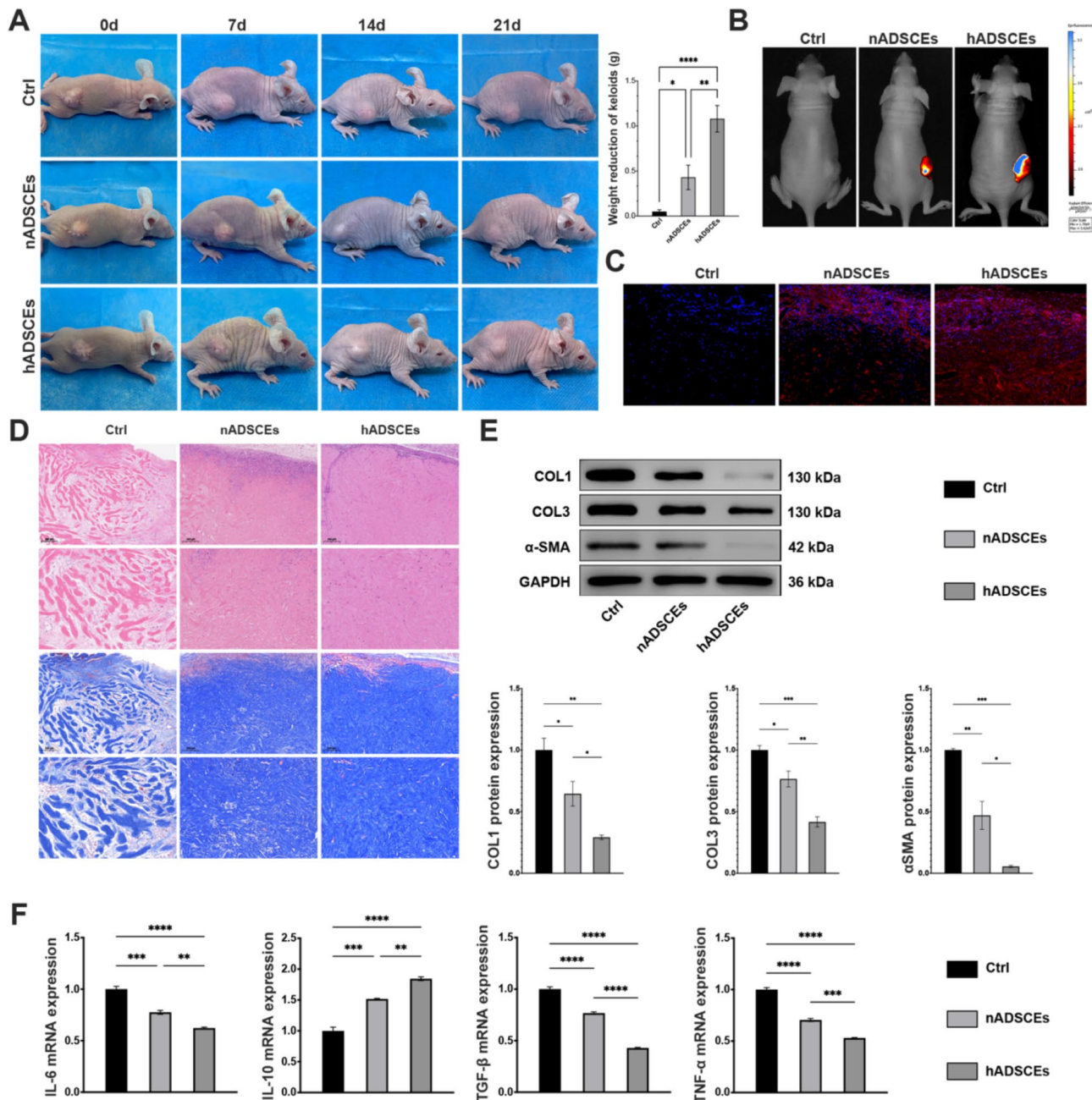


**Fig. 5** Effects of ADSC exosomes treatment on graft quality and pathological changes. **(A)** Photographs of keloids were taken at 0, 7, 14 and 21 days after implantation, and the transplants were taken out at 21 days and weighed. **(B)** An animal imaging system was used. **(C)** nADSCs and hADSCs stained with PKH26 were injected into the keloid graft of model mice, and the keloids were observed by fluorescence microscope after 7 days. **(D)** HE and Masson staining of keloids. **(E)** Western blot analysis of COL1, COL3, and  $\alpha$ SMA protein levels in the animal model. **(F)** Changes in the mRNA levels of the inflammatory factors IL-6 and IL-10, TGF- $\beta$ 1 and TNF- $\alpha$  after treatment with nADSCs and hADSCs. Full-length blots are presented in Supplementary Fig. 4

aggregates (Fig. 5D). Moreover, western blot data showed that the ADSC exosomes downregulated the expression of COL11, COL3 and  $\alpha$ SMA (Fig. 5E). In addition, RT-PCR analysis also showed that ADSC exosomes downregulated the mRNA expression of TGF- $\beta$ 1, TNF- $\alpha$ , and IL-6 and upregulated the mRNA expression of IL-10 in keloid tissue (Fig. 5F). These findings indicated that ADSC exosomes suppressed chronic inflammation in keloid tissue, significantly reduced collagen deposition in keloids, and attenuated fibrosis.

#### ADSC exosomes promote mitochondrial autophagy and restore damaged mitochondrial morphology in a mouse model of keloid scarring

To investigate the molecular mechanism underlying the effects of ADSC exosomes treatment on keloids in vivo, western blot was used to analyze the phosphorylation level of components of the PI3K/AKT/mTOR pathway in the keloid grafts of each group, and the results showed that in the human keloid implantation model, ADSC exosomes significantly inhibited the phosphorylation of components of the PI3K/AKT/mTOR pathway at the keloid tissue level (Fig. 6A), which strongly suggested that in vivo, ADSCs may exert therapeutic effects by inhibiting the PI3K/AKT/mTOR pathway. The western blot results were consistent with the results of the in

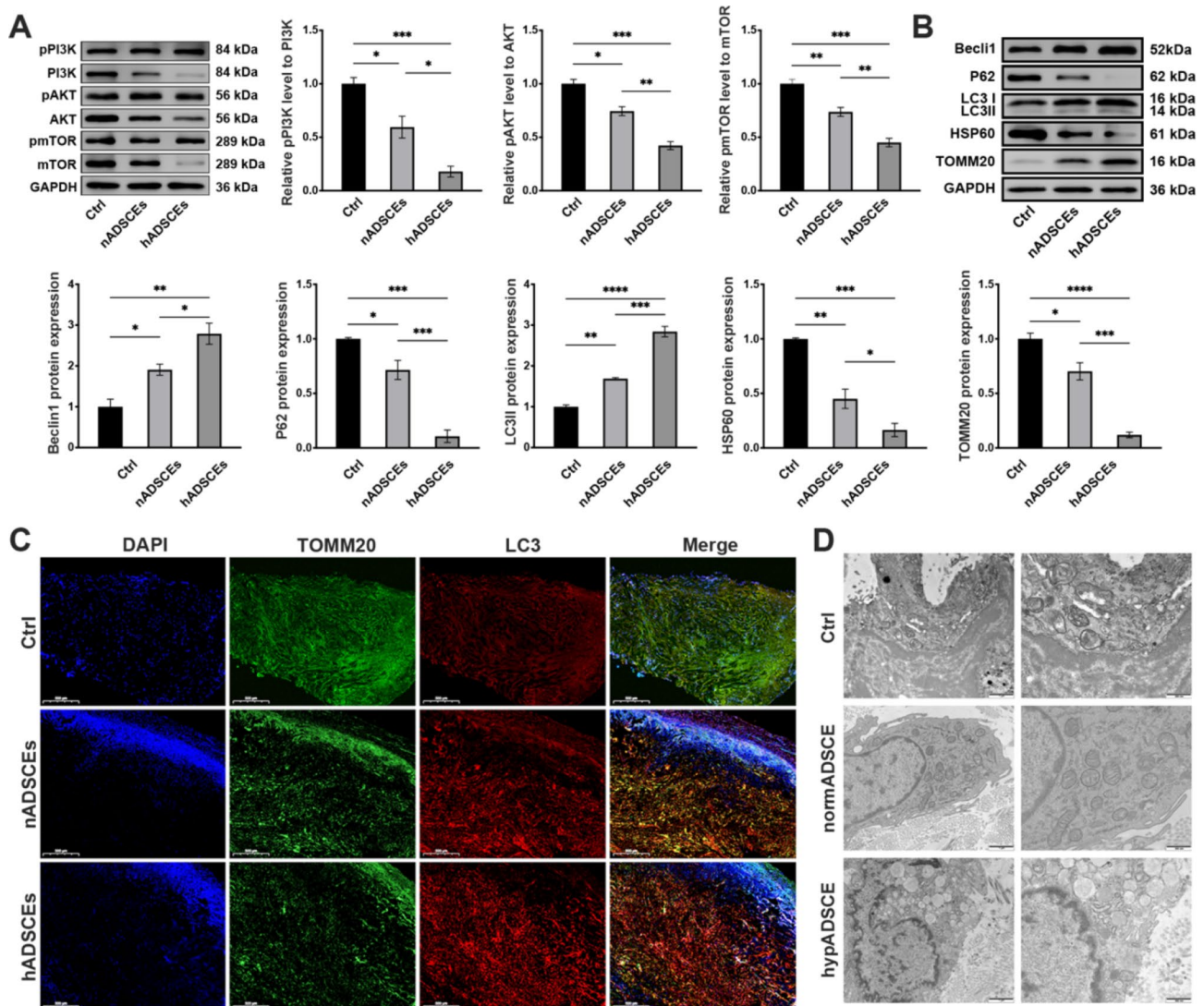


**Fig. 6** ADSC exosomes promote mitochondrial autophagy in vivo. **(A)** The phosphorylation level of components of the PI3K/AKT/mTOR pathway components in keloids was assessed by western blotting. **(B)** Assessment of the protein levels of the autophagy-related proteins Beclin1, P62, and LC3 and the mitochondria-related proteins HSP60 and TOMM20 in keloids. **(C)** The expression of LC3 and TOMM20 in animal model keloid tissue. **(D)** Observation of the morphological alterations of mitochondria in keloid scars by electron microscopy. Full-length blots are presented in Supplementary Fig. 5



vitro experiments. In keloid tissues, P62 and LC3II/LC3I levels increased after ADSC exosomes treatment, and Beclin1, HSP60, and Tomm20 levels decreased; additionally, the effects of treatment with hADSCs was superior to effects of treatment with nADSCs (Fig. 6B). Moreover, we fluorescently stained the grafts to assess P62 and Tomm20 expression (Fig. 6C). These findings suggested that *in vivo*, ADSC exosomes likely promote mitochondrial autophagy in keloids. To observe the change in mitochondrial morphology in keloid tissue, transmission electron microscopy was used, and the mitochondria in the control group exhibited an abnormal vacuole morphology and ridge breaks, with almost no normal mitochondria. In contrast, after ADSC exosomes treatment, a certain number of mitochondria with normal morphology were observed (Fig. 6D).

## Discussion

Keloid scarring is a poor outcome of abnormal wound healing, and effective drugs against keloid scarring are urgently needed [11]. In this study, we demonstrated that ADSC exosomes significantly alleviate keloids by promoting mitochondrial autophagy in KFs. In addition, the therapeutic effect of hypoxia-treated ADSC exosomes appeared to be greater than that of exosomes secreted by ADSCs under normoxia. These findings suggest that ADSC exosomes may be a novel therapeutic option for the treatment of keloids.

Recently, adipose stem cell-based therapies have been shown to be effective for the treatment of keloids [31, 32]. Previous studies have shown that adipose stem cell exosomes play a central role in reducing chronic inflammation in keloid fibroblasts and attenuating fibrosis [33]. TSG-6 in ADSC exosomes prevents keloid scar formation by reducing inflammation and inhibiting collagen deposition enhanced in keloids by TGF- $\beta$ , a key cytokine in the regulation of keloid fibrosis which promotes collagen synthesis and prevents its degradation [34, 35]. Studies have shown that fetal scarless wounds expressed high levels of TGF- $\beta$ 3 and low levels of TGF- $\beta$ 1 and TGF- $\beta$ 2 [36]. In addition, bone marrow mesenchymal stem cells reduce fibrosis by reducing the ratio of TGF- $\beta$ 1/ TGF- $\beta$ 3 of wound lysate in mouse full-thickness wound healing model [7]. ADSC exosomes promote the proliferation and migration of fibroblasts from normal skin, thereby accelerating diabetic wound healing. Moreover, under hypoxic condition, adipose stem cells secrete more exosomes to improve tissue and blood perfusion in hypoxic environments and reduce inflammatory infiltration in fat [37]. Compared with those under normoxic condition, adipose stem cell exosomes under hypoxic condition are more effective at promoting angiogenesis and bone healing and accelerating diabetic wound healing [30, 38, 39]; this suggests that hypoxia-derived adipose stem cell

exosomes may be more advantageous for disease treatment. In this study, we applied both nADSCs and hADSCs to treat KFs and keloid model mice, and the results showed that hADSCs were better able to inhibit the proliferation, migration, and collagen deposition of KFs, reduce the weight of keloid grafts, and attenuate the level of collagen deposition and fibrosis. These findings demonstrated that adipose stem cell exosomes under hypoxic condition were more effective than adipose stem cell exosomes under normoxic condition at treating keloid scars.

Through bulk RNA sequencing and bioinformatics analysis, it was found that keloid scars transcriptionally differed from normal and hypertrophic scars [40]. Hyperactivation of the PI3K/AKT/mTOR pathway in keloids plays a key role in the excessive proliferation of keloid fibroblasts and abnormal collagen deposition [41, 42]. Compared with normal dermal-derived fibroblasts, keloid-derived fibroblasts exhibit decreased autophagic flux, P62 aggregation and interactions with LC3 [23]. Defects in the autophagic protein Beclin1 increase collagen deposition and promote a profibrotic phenotype in the mouse kidney [43]. Thus, the PI3K/AKT/mTOR pathway and p62/LC3 signaling are involved in the development of keloidogenic autophagy dysfunction and fibrosis. Compared with normal dermal tissue, keloid tissue contains damaged low-density mitochondria and ridge breaks [23]. In renal fibrosis, the promotion of mitochondrial autophagy and improvements in mitochondrial function effectively alleviate renal fibrosis [44]. Increases in mitochondrial oxidative stress and mitochondrial dysfunction are associated with the pathogenesis of keloid scars. In this study, ADSC-derived exosomes were applied to KFs and keloid model mice, and activation of the PI3K/AKT/mTOR pathway, expression of p62, and enhancement of the LC3 II/LC3 I ratio were significantly suppressed, mitochondrial morphology and function were restored, and colocalization of mitochondria and lysosomes was increased, suggesting that ADSCs are involved in promoting keloid fibroblast mitochondrial autophagy *in vivo* and restoring mitochondrial morphology and function.

There are some limitations of our experiments. For example, promoting mitochondrial autophagy may not be the only mechanism by which ADSC exosomes affect autophagic flow in keloid fibroblasts, which needs to be investigated through subsequent experiments. Differences in the effect of ADSC exosomes on keloid fibroblasts in different parts of the human body and different spatial distributions of keloid fibroblasts in keloid tissue may be identified by spatiotemporal proteomic sequencing of keloid fibroblasts originating from different body parts and with different spatial distributions.



## Conclusion

ADSC exosomes can exist stably in keloid tissue, and promote mitochondrial autophagy to play a therapeutic role through PI3K/AKT/mTOR pathway. Meanwhile, both nADSCEs and hADSCEs could treat keloids, but hADSCEs were more effective.

## Abbreviations

ADSCs	Adipose stem cells
AKT	Protein Kinase B
COL1	Collagen type I
COL3	Collagen type III
hADSCEs	hypoxic adipose stem cell exosomes
HUVECs	Human umbilical vein endothelial cells
IL10	Interleukin 10
IL-6	Interleukin 6
KFs	Keloids
mTOR	mammalian target of rapamycin
nADSCEs	normoxic adipose stem cell exosomes
PI3k	Phosphatidylinositol 3-kinases
TGF-β	Transforming growth factor-β
TNF-α	Tumor necrosis factor-α

## Supplementary Information

The online version contains supplementary material available at <https://doi.org/10.1186/s13287-024-03928-5>.

Supplementary Material 1

## Acknowledgements

The authors declare that they have not used AI-generated work in this manuscript in this section.

## Author contributions

ZX, CL and LK designed experiments. CL and LK FL prepared the exosomes, performed the experiments, and contributed to writing the manuscript. YQ, YZ analyzed the experimental data. All authors listed reviewed the paper and provided feedback. All authors read and approved the final manuscript.

## Funding

The work was supported by Central Financial Support Fund for the Reform and Development of Local Colleges (Grant 2021-理工类-高水平人才13), National Natural Science Foundation of China (Grant No. 81471796), Excellent Youth Foundation of Heilongjiang Province of China (Grant JC2017019), and Scientific Research Innovation Project of Harbin Medical University (Grant YJSCX2020-39HYD).

## Data availability

We confirmed that the research scheme including research questions, key design features and analysis plan had been prepared before the experiment, and the scheme had been registered in the Second Affiliated Hospital of Harbin Medical University. Relevant data are included in the article and its supplementary materials or are available from the corresponding author upon reasonable request.

## Declarations

### Ethics approval and consent to participate

This study was approved by the Institutional Review Board of the Second Hospital of Harbin Medical University (Approval number: YJSKY2022-346, Date of approval: August 23, 2022) and adhered to the tenants of the Declaration of Helsinki. The patients provided written informed consent for the use of the samples. The animal experiment was approved by the Animal Ethical Committee of the Second Hospital of Harbin Medical University (Approval number: SYDW2022-188, Date of approval: August 23, 2022). Title of the approved project for both animal and human studies: Adipose stem cell exosomes inhibit keloids through PI3K/AKT pathway. All operations involving

animal experiments in this experiment strictly follow the guidelines outlined in the revised Animals (Scientific Procedures) Act 1986 in the UK and Directive 2010/63/EU in Europe.

### Consent for publication

All authors consent for publication.

### Competing interests

The author(s) declare no competing interests.

### Author details

<sup>1</sup>Department of Plastic and Aesthetic Surgery, The Second Affiliated Hospital of Harbin Medical University, Harbin 150081, China

Received: 6 August 2024 / Accepted: 5 September 2024

Published online: 15 September 2024

## References

1. Diaz A, et al. Keloid lesions show increased IL-4/IL-13 signaling and respond to Th2-targeting dupilumab therapy. *J Eur Acad Dermatol Venereol*. 2020;34:e161–4.
2. Arno AI, Gauglitz GG, Barret JP, Jeschke MG. Up-to-date approach to manage keloids and hypertrophic scars: a useful guide. *Burns*. 2014;40:1255–66.
3. Kashiwama K, et al. miR-196a downregulation increases the expression of type I and III collagens in keloid fibroblasts. *J Invest Dermatol*. 2012;132:1597–604.
4. Lee S-Y, et al. IL-17 induces Autophagy Dysfunction to promote inflammatory cell death and fibrosis in keloid fibroblasts via the STAT3 and HIF-1α Dependent Signaling pathways. *Front Immunol*. 2022;13:888719.
5. Chao H, et al. IL-13RA2 downregulation in fibroblasts promotes keloid fibrosis via JAK/STAT6 activation. *JCI Insight*. 2023;8:e157091.
6. Del Principe D, Lista P, Malorni W, Giammarioli AM. Fibroblast autophagy in fibrotic disorders. *J Pathol*. 2013;229:208–20.
7. Tsai C-H, Ogawa R. Keloid research: current status and future directions. *Scars Burn Heal*. 2019;5:2059513119868659.
8. Ogawa R. Surgery for scar revision and reduction: from primary closure to flap surgery. *Burns Trauma*. 2019;7:7.
9. Li K, et al. The 1470 nm diode laser with an intralesional fiber device: a proposed solution for the treatment of inflamed and infected keloids. *Burns Trauma*. 2019;7:5.
10. Jafarzadeh A, PourMohammad A, Goodarzi A. A systematic review of the efficacy, safety and satisfaction of regenerative medicine treatments, including platelet-rich plasma, stromal vascular fraction and stem cell-conditioned medium for hypertrophic scars and keloids. *Int Wound J*. 2024;21:e14557.
11. Ekstein SF, Wyles SP, Moran SL, Meves A. Keloids: a review of therapeutic management. *Int J Dermatol*. 2021;60:661–71.
12. Park J, Kim Y-C. Topical delivery of 5-fluorouracil-loaded carboxymethyl chitosan nanoparticles using microneedles for keloid treatment. *Drug Deliv Transl Res*. 2021;11:205–13.
13. Dhurat R, Daruwalla SB, Sharma A. Fractionated devolumizing keloid tissue: the 'pop' method: a novel technique to facilitate administration of intral-lesional corticosteroid in difficult keloids. *J Am Acad Dermatol*. 2023;88:e75–7.
14. Wang X, Ma Y, Gao Z, Yang J. Human adipose-derived stem cells inhibit bioactivity of keloid fibroblasts. *Stem Cell Res Ther*. 2018;9:40.
15. Liu S, et al. Mesenchymal stem cells prevent hypertrophic scar formation via inflammatory regulation when undergoing apoptosis. *J Invest Dermatol*. 2014;134:2648–57.
16. Lee S-Y, et al. IL-17 Induced Stromal Cell-Derived Factor-1 and profibrotic factor in keloid-derived skin fibroblasts via the STAT3 pathway. *Inflammation*. 2020;43:664–72.
17. Lichtman MK, Otero-Vinas M, Falanga V. Transforming growth factor beta (TGF-β) isoforms in wound healing and fibrosis. *Wound Repair Regen*. 2016;24:215–22.
18. Bray K, et al. Autophagy suppresses RIP kinase-dependent necrosis enabling survival to mTOR inhibition. *PLoS ONE*. 2012;7:e41831.
19. Xue L, Fletcher GC, Tolkovsky AM. Mitochondria are selectively eliminated from eukaryotic cells after blockade of caspases during apoptosis. *Curr Biol*. 2001;11:361–5.
20. Bharath LP, et al. Metformin enhances autophagy and normalizes mitochondrial function to Alleviate Aging-Associated inflammation. *Cell Metab*. 2020;32:44–e556.

21. Hill C, et al. Autophagy inhibition-mediated epithelial-mesenchymal transition augments local myofibroblast differentiation in pulmonary fibrosis. *Cell Death Dis.* 2019;10:591.
22. Shiekh PA, Singh A, Kumar A. Exosome laden oxygen releasing antioxidant and antibacterial cryogel wound dressing OxOBand alleviate diabetic and infectious wound healing. *Biomaterials.* 2020;249:120020.
23. Wang Q, et al. Altered glucose metabolism and cell function in keloid fibroblasts under hypoxia. *Redox Biol.* 2021;38:101815.
24. Do DV, et al. Interleukin-18 system plays an important role in keloid pathogenesis via epithelial-mesenchymal interactions. *Br J Dermatol.* 2012;166:1275–88.
25. Xin Y, Min P, Xu H, Zhang Z, Zhang Y. CD26 upregulates proliferation and invasion in keloid fibroblasts through an IGF-1-induced PI3K/AKT/mTOR pathway. *Burns Trauma* 8, (2020).
26. Andreoli A, Ruf MT, Itin P, Pluschke G, Schmid P. Phosphorylation of the ribosomal protein S6, a marker of mTOR (mammalian target of rapamycin) pathway activation, is strongly increased in hypertrophic scars and keloids. *Br J Dermatol.* 2015;172:1415–7.
27. Mazini L, Rochette L, Admou B, Amal S, Malka G. Hopes and limits of adipose-derived stem cells (ADSCs) and mesenchymal stem cells (MSCs) in Wound Healing. *Int J Mol Sci.* 2020;21:1306.
28. Zhao B, et al. Exosomes derived from human amniotic epithelial cells accelerate wound healing and inhibit scar formation. *J Mol Histol.* 2017;48:121–32.
29. Zhang Y et al. Exosomes Derived from Adipose Mesenchymal Stem Cells Promote Diabetic Chronic Wound Healing through SIRT3/SOD2. *Cells* 11, 2568 (2022).
30. Wang J, et al. Hypoxia adipose stem cell-derived exosomes promote high-quality healing of diabetic wound involves activation of PI3K/Akt pathways. *J Nanobiotechnol.* 2021;19:202.
31. Chen H, Hou K, Wu Y, Liu Z. Use of adipose stem cells against hypertrophic scarring or keloid. *Front Cell Dev Biol.* 2021;9:823694.
32. Yang J, Li S, He L, Chen M. Adipose-derived stem cells inhibit dermal fibroblast growth and induce apoptosis in keloids through the arachidonic acid-derived cyclooxygenase-2/prostaglandin E2 cascade by paracrine. *Burns Trauma.* 2021;9:tkab020.
33. Li J, Li Z, Wang S, Bi J, Huo R. Exosomes from human adipose-derived mesenchymal stem cells inhibit production of extracellular matrix in keloid fibroblasts via downregulating transforming growth factor- $\beta$ 2 and Notch-1 expression. *Bioengineered.* 2022;13:8515–25.
34. Li Y, et al. Cryptotanshinone downregulates the profibrotic activities of hypertrophic scar fibroblasts and accelerates wound healing: a potential therapy for the reduction of skin scarring. *Biomed Pharmacother.* 2016;80:80–6.
35. Jiang L, et al. Exosomes derived from TSG-6 modified mesenchymal stromal cells attenuate scar formation during wound healing. *Biochimie.* 2020;177:40–9.
36. Occlleston NL, et al. Discovery and development of avotermin (recombinant human transforming growth factor beta 3): a new class of prophylactic therapeutic for the improvement of scarring. *Wound Repair Regen.* 2011;19(Suppl 1):s38–48.
37. Han Y, et al. Co-transplantation of exosomes derived from hypoxia-preconditioned adipose mesenchymal stem cells promotes neovascularization and graft survival in fat grafting. *Biochem Biophys Res Commun.* 2018;497:305–12.
38. Liu W, et al. Melatonin-stimulated MSC-derived exosomes improve diabetic wound healing through regulating macrophage M1 and M2 polarization by targeting the PTEN/AKT pathway. *Stem Cell Res Ther.* 2020;11:259.
39. Xue C, et al. Exosomes derived from hypoxia-treated human adipose mesenchymal stem cells enhance Angiogenesis through the PKA Signaling Pathway. *Stem Cells Dev.* 2018;27:456–65.
40. Walter AS, et al. Keloids are transcriptionally distinct from normal and hypertrophic scars. *Eur J Dermatol.* 2023;33:604–11.
41. Tu T, et al. CUDC-907 reverses pathological phenotype of keloid fibroblasts in vitro and in vivo via dual inhibition of PI3K/Akt/mTOR signaling and HDAC2. *Int J Mol Med.* 2019;44:1789–800.
42. Lv D, et al. S-Nitrosylation-mediated coupling of DJ-1 with PTEN induces PI3K/AKT/mTOR pathway-dependent keloid formation. *Burns Trauma.* 2023;11:tkad024.
43. Ding Y, et al. Autophagy regulates TGF- $\beta$  expression and suppresses kidney fibrosis induced by unilateral ureteral obstruction. *J Am Soc Nephrol.* 2014;25:2835–46.
44. Wang Yet al. LYC inhibits the AKT signaling pathway to activate autophagy and ameliorate TGF $\beta$ -induced renal fibrosis. *Autophagy.* 2023;1–20

#### Publisher's note

Springer Nature remains neutral with regard to jurisdictional claims in published maps and institutional affiliations.